Electromagnetic Analysis of Nanoscale Heterogeneity
The Domain-Integrated Perspective

Lager, Ioan E.; Vandenbosch, Guy A.E.; Stumpf, Martin

DOI
10.23919/EuMC.2018.8541698

Publication date
2018

Document Version
Accepted author manuscript

Published in
2018 48th European Microwave Conference, EuMC 2018

Electromagnetic analysis of nanoscale heterogeneity – the domain-integrated perspective –

Ioan E. Lager
Faculty of Electrical Engineering,
Mathematics and Computer Science
Delft University of Technology
Mekelweg 4, 2628 CD Delft, the Netherlands
Email: i.e.lager@tudelft.nl

Guy A. E. Vandenbosch
Electrical Engineering Dpt., TELEMIC
Katholieke Universiteit Leuven
Kasteelpark Arenberg 10 bus 2444
B-3001 Leuven, Belgium
Email: guy.vandenbosch@kuleuven.be

Martin Štumpf
SIX Research Centre
Brno University of Technology
Technická 3082/12,
616 00 Brno, the Czech Republic
Email: martin.stumpf@centrum.cz

***Abstract*—This paper introduces a new paradigm in the electromagnetic (EM) analysis of largely inhomogeneous nanostructures. It is shown that the high degree of inhomogeneity may render the traditional discretisation of such topologies problematic. A new discretisation scheme that is much better matched to these topologies is proposed. The scheme involves a more adequate meshing and discretisation formalism, in conjunction with an original combination of dual space-time EM field quantities to be calculated. The pivotal field equations are elaborately discussed, with an emphasis on their computational implications.**

I. Introduction

The versatility and (relative) affordability of commercial computational EM (CCEM), CST Microwave Studio (CST) and ANSYS – High Frequency Electromagnetic Field Simulation (HFSS) in the first place, 'democratised' the use of such instruments to the point where CCEM is presently presumed in *any* EM (related) research and became an almost standard tool in EM (related) curricula [1]. The prevalence of CCEM puts self-developed codes under pressure, such codes being now exclusively the teritory of extremely specialised studies and, highly relevantly, being assessed against the same CCEM tools (construed as some sort of 'golden standards').

Can we compete with CCEM? For most simulation tasks, the answer is, probably, "no". Nonetheless, nanotechnologies (*e.g.*, nanospheres, nanodipoles or dimers becoming critical enablers as optical antennas [2]–[4]), emerging carbon-based nanoelectronics [5], or applications beyond 1 THz that become increasingly less exotic, *may* demand different approaches for a twofold reason: (i) technically, EM analysis of nanoparticles may push general-purpose codes beyond their limits and (ii) more importantly, researchers must become more aware of the computational results' relevance – to quote Professor de Hoop: "A code will always yield some numbers.".

This paper advocates a novel viewpoint in the computational EM (CEM) analysis at nanoscale level. By starting from the fundamental works [6]–[10] and a selection of verified strategies [11]–[17] it will propose an approach that is deemed highly opportune for tackling nanoscale inhomogeneity.

II. Global framework

EM modelling of nanoscale inhomogeneity brings EM analysis at scales that approach the limit of validity of the *macroscopic EM laws* (see [18, pp. 286–289] for this lower bound). Moreover, this is also the limit at which *macroscopic measurements* are still feasible. In line with [15], [17], we term this scale as the *mesoscopic scale*.

Two aspects are crucial: (a) inhomogeneity is maintained in the envisaged configurations down to the mesoscopic scale and (b) a subdivision beyond that scale, *although computationally perfectly possible*, cannot be justified physically. These arguments recommend choosing the mesoscopic scale as the scale of the discretisation in a mesh-based CEM scheme. In the case of *bounded domain* techniques, *e.g.*, the Finite Integration Technique (FIT) [6] (at the core of CST) or the Finite-Element Method (FEM) [19] (at the core of HFSS), the mesh should fit the boundaries of the (often highly) contrasting subdomains of the configuration. However, FIT is known to suffer from the effect of staggered grids with *non-coinciding* electric and magnetic interfaces. Precluding the fuzziness of the resulting interfaces requires sub-meshing mesoscopic subdomains, often over very thin sheets, the employed material parameters having then little physical background on grounds of the observation (b) above. To the best of our knowledge, FEM too suffers from similar impediments. Moreover, depending on the discretisation of physical quantities at hand [7], [8], [12], [20], some EM field quantities may also be poorly represented.

By starting from the *domain-integrated method*, the CEM formalism introduced in [17, Section VI] offers a viable solution to this deadlock. The prerequisites will be:

- Construct a *simplicial* mesh at mesoscopic scale – tight-fit the mesh on the boundaries of the subdomains where material continuity can be assumed and sub-mesh those subdomains only inasmuch as the geometry demands it such that to be able to perform a Delaunay meshing.
- Discretise EM field quantities via consistently linear edge and face expansion functions [7]. A possible combination of such expansion functions with standard Cartesian ones (with [16], [21] offering the path to follow) may be considered for increased computational effectiveness.

The choice for EM quantities and their discretisation will be henceforth elaborated upon. These quantities will then be used in a set of EM field equations that can be directly transferred

into a computational scheme. The last step will be to describe that numerical strategy and analyse its (possible) limitations.

III. Field quantities

A vast bibliography [9]–[14], [20], [22], [23] conclusively proves that *complementarity* is indispensable to constructing consistent CEM formulations. Our starting point is the twofold perspective on complementarity in [9], [10], with specific *types* of EM quantities being associated with specific *supports* – in a numerical scheme, these are the elements of a (simplicial) mesh. Based on energetic arguments, Tonti distinguishes between configuration ↔ source EM *integral* field quantities that are associated with supports having inner ↔ outer geometric orientations. This reasoning dictates the use of *dual meshes* for representing EM field quantities and laws.

Tonti's view was at the crux of the choices in [17]. Most of those choices are taken over in the present proposal:

1) Use a simplicial (tetrahedral) mesh as a *primal mesh* and its barycentric dual (see Fig. 1) as a *dual mesh*.
2) Use the *local* EM field quantities: electric field strength $\boldsymbol{E}(\boldsymbol{r},t)$, electric flux density $\boldsymbol{D}(\boldsymbol{r},t)$, magnetic field strength $\boldsymbol{H}(\boldsymbol{r},t)$ and magnetic flux density $\boldsymbol{B}(\boldsymbol{r},t)$[†].
3) The local EM field quantities *are expanded on the primal mesh, only* – the employed expansion technique must be consistent with the interface boundary conditions applying to the relevant local field quantities. Complement the spatial discretisation by a linear time discretisation.
4) The field quantities are defined on the boundary of the simplicial cells, only. Those values are *extrapolated* into the cells' interior (algebraic topology ensures the possibility to employ a consistently linear spatial expansion, based on the limiting values of the expanded quantities upon approaching nodes, edges and faces). This procedure allows performing line, surface and volume integrations of the local EM field quantities.
5) Employ the *integral field relations* (1) and (2) below on the boundaries of space–time elements. These equations make no reference to properties of the matter.
6) Use the relations (3) and (4) below for constructing constitutive relations via volume energy minimisation. Use these constitutive relations for deriving mappings of the expansion coefficients pertaining to the relevant complementary quantities.

The cardinal difference between the present proposal and that in [17] is in the choice for the complementary quantities to be computed. The approach in [17] used to this end $\boldsymbol{E}(\boldsymbol{r},t)$ and $\boldsymbol{H}(\boldsymbol{r},t)$, primarily for computational effectiveness, but also because that was the choice in [7] and in the therefrom developed methods. However, there are solid theoretical and practical reasons for using $\boldsymbol{E}(\boldsymbol{r},t)$ and $\boldsymbol{B}(\boldsymbol{r},t)$ instead:

- Starting from special relativity theory arguments, it can be inferred that $\boldsymbol{E}$ and $\boldsymbol{B}$ are the fundamental EM field quantities and not $\boldsymbol{E}$ and $\boldsymbol{H}$ [24, p. 477].
- Operating with $\boldsymbol{E}$ and $\boldsymbol{B}$ entails evaluating exclusively field quantities that are continuous across *any* (locally) smooth interface. Note that any *imposed* discontinuity of their applicable field components requires invoking active magnetic charge distributions or currents ("active" being interpreted as in [26, Section 18.3]). While "induced" magnetic charges or currents may serve a purpose in CEM (not in our scheme), *imposing* them requires acknowledging their physical existence and all available observations compellingly contradict this. On the contrary, $\boldsymbol{H}$ and $\boldsymbol{D}$ are allowed to show jump discontinuities (in a limiting sense) due to electric currents or charge distributions inside domains of vanishing thickness.
- In conjunction with the type of field representation advocated above, selecting the continuous quantities $\boldsymbol{E}$ and $\boldsymbol{B}$ as computational quantities alleviates the modelling of interfaces – an exceptionally testing programming task for the considered highly inhomogeneous configurations.

It is noted that, at first glance, our choice seems incapable of handling surface electric currents and electric charge distributions. To begin with, our mesoscopic scale analysis all but excludes the possibility of physically justifiable electric features manifesting inside domains of significantly smaller thicknesses. Should our method be applied at a scale where such surface distributions still make sense, these features *can* be accounted for by interrelating the expansion coefficients of $\boldsymbol{H}$ and $\boldsymbol{D}$. These coefficients will not be directly calculated, but the relevant contributions will eventually turn up in the calculated quantities via the mappings induced by the constitutive relations. It is stressed that including these jump discontinuities will entail serious complications in the coding of such situations and in the underlying mesh and degrees of freedom (DoFs) databases. From this perspective, it seems desirable to transfer surface distributions into volume ones that can be handled easier. To conclude with, [22] too uses an $\boldsymbol{E}$ – $\boldsymbol{B}$ dual representation, with $\boldsymbol{E}$ being discretised on a primal mesh and $\boldsymbol{B}$ on a dual one (as in the case of FIT – see the observation on modelling interfaces in Section II).

IV. Integral EM field equations

In line with [17], the selected local expansions are used in *integral field relations*. By using the notations: $\mathcal{D}$ = a bounded domain with piecewise smooth boundary $\partial\mathcal{D}$, $\mathcal{S}$ = a simply connected subsurface of $\partial\mathcal{D}$ with piecewise smooth boundary $\partial\mathcal{S}$, $\boldsymbol{n}$ = the unit vector along the outward normal to $\partial\mathcal{D}$ (the orientation on $\partial\mathcal{S}$ and that of $\boldsymbol{n}$ are related by means of the screw rule), $\boldsymbol{\tau}$ = the unit vector along the tangent to $\partial\mathcal{S}$, and $\mathcal{T}$ = a bounded time interval with boundary $\partial\mathcal{T}=\{t_1,t_2\}$, the space-time domain-integrated field relations are [15], [17]

$$\int_{\partial\mathcal{S}\times\mathcal{T}} \boldsymbol{\tau}\cdot\boldsymbol{E}(\boldsymbol{r},t)\,\mathrm{d}L\mathrm{d}t + \int_{\mathcal{S}} \boldsymbol{n}\cdot\boldsymbol{B}(\boldsymbol{r},t)\,\mathrm{d}A\Big|_{\partial\mathcal{T}} = 0 \quad (1)$$

$$\int_{\partial\mathcal{S}\times\mathcal{T}} \boldsymbol{\tau}\cdot\boldsymbol{H}(\boldsymbol{r},t)\,\mathrm{d}L\mathrm{d}t - \int_{\mathcal{S}} \boldsymbol{n}\cdot\boldsymbol{D}(\boldsymbol{r},t)\,\mathrm{d}A\Big|_{\partial\mathcal{T}} = 0. \quad (2)$$

[†]Position in the configuration is specified by the coordinates $\{x,y,z\}$ with respect to a background Cartesian reference frame with origin O and three mutually orthogonal unit vectors $\{\hat{\boldsymbol{x}},\hat{\boldsymbol{y}},\hat{\boldsymbol{z}}\}$ that, in this order, form a right-handed system. The position vector is $\boldsymbol{r} = x\hat{\boldsymbol{x}} + y\hat{\boldsymbol{y}} + z\hat{\boldsymbol{z}}$, with $|\boldsymbol{r}| = r$. The time coordinate is t.

These relations are supplemented with the following volume (source) integral relations

$$\int_{\partial\mathcal{D}} \boldsymbol{n}\cdot\boldsymbol{B}(\boldsymbol{r},t)\mathrm{d}A\Big|_{\partial\mathcal{T}} = 0 \tag{3}$$

$$\int_{\partial\mathcal{D}} \boldsymbol{n}\cdot\boldsymbol{D}(\boldsymbol{r},t)\mathrm{d}A\Big|_{\partial\mathcal{T}} = 0 \tag{4}$$

where $\Big|_{\partial\mathcal{T}}$ stands for $f(t)\Big|_{\partial\mathcal{T}} = f(t_2) - f(t_1)$. Equations (3) and (4) generalise the standard Gauss's laws but, as stressed in [17], they are, in fact, space-time integrated compatibility relations since a summation of (1) and (2) applied to any subsurface composing $\partial\mathcal{D}$ yields *automatically* (3) and (4).

Two important observations can be made with respect to these space-time domain-integrated relations:

1) In line with [9], [10], (1) and (3) are written for curves and surfaces with an *inner orientation*, while (2) and (4) for curves and surfaces with an *outer orientation*. In our computational scheme, this will have an impact on the choice for the supports of the relevant integrals.
2) Relations (1), (3) have the dimension of action rated by charge and (2), (4) that of charge – in physics, action and charge are the fundamental *mechanical* and *electrical* 'physical observables' [25], respectively. In this sense, it is noted that [18, p. 273] speculated on the benefits (and beauty) of a CEM method using action as basic quantity and observed the non-availability of such a formulation. Our proposal may offer that missing tool.

V. Computational Approach

The principles and tools introduced in Sections II–IV are now assembled into a CEM scheme. This formalism uses a simplicial decomposition of the domain of computation, with the simplicial mesh providing the *primal grid* and its barycentric dual the *dual grid*. This situation is illustrated in Fig. 1 that shows the simplicial star of an edge $\overrightarrow{\mathcal{N}_0\mathcal{N}_7}$ and (a part of) its barycentric dual. The pertaining tetrahedra, with the relevant parts of the barycentric dual, are also represented separately. The picture of $\mathcal{T}_1$ also contains the remaining facets of the complete barycentric dual surface enclosing the node $\mathcal{N}_0$. By using [17] as a guideline, we opt for the followings:

1) Relations of type (1) are written for closed contours along the *primal mesh*, enclosing the nodes where $\boldsymbol{E}$ is unknown (for example, the contour ∂S in Fig. 1 for the unknown edge coefficient corresponding to the edge $\overrightarrow{\mathcal{N}_0\mathcal{N}_7}$, at $\mathcal{N}_0$). Note that the expansions of $\boldsymbol{B}$ on the facetted surface $\mathcal{S}$ are readily available. Moreover, by summing all $\boldsymbol{B}$ expansions on the complete simplicial star of the edge $\overrightarrow{\mathcal{N}_0\mathcal{N}_7}$, (3) is automatically satisfied.
2) Relations of type (2) are written for closed contours along the *dual mesh*, like the contour $\{\mathrm{a},\mathrm{b},\mathrm{c},\mathrm{d},\mathrm{e},\mathrm{f},\mathrm{a},\}$ in Fig. 1. Since only expansions of $\boldsymbol{D}$ on the primal mesh are available, the needed surface integrals are derived from corresponding closed surface integrals on surfaces such as the boundary of the polyhedron with vertices $\{\mathcal{N}_0,\mathrm{a},\mathrm{b},\mathrm{c},\mathrm{d},\mathrm{e},\mathrm{f},\mathrm{a}\}$. Note that, by combining relations of the type (2) written for all 4 subregions of $\mathcal{T}_1$, (4), when applied to $\mathcal{T}_1$, is automatically satisfied.
3) These relations are supplemented by $\boldsymbol{D}\leftrightarrow\{\boldsymbol{E},\boldsymbol{P}\}$ and $\boldsymbol{B}\leftrightarrow\{\boldsymbol{H},\boldsymbol{M}\}$ mappings that follow from the constitutive relations, with $\boldsymbol{P}$ and $\boldsymbol{M}$ denoting the impressed electric polarisation and magnetisation, respectively‡.
4) The DoFs associated with $\boldsymbol{E}$ and $\boldsymbol{B}$ are kept, while those associated with $\boldsymbol{H}$ and $\boldsymbol{D}$ are eliminated via the mappings provided by the constitutive relations (see also [22]), possibly supplemented by relations following from jump discontinuities at interfaces where surface electric currents or charge distributions are present.

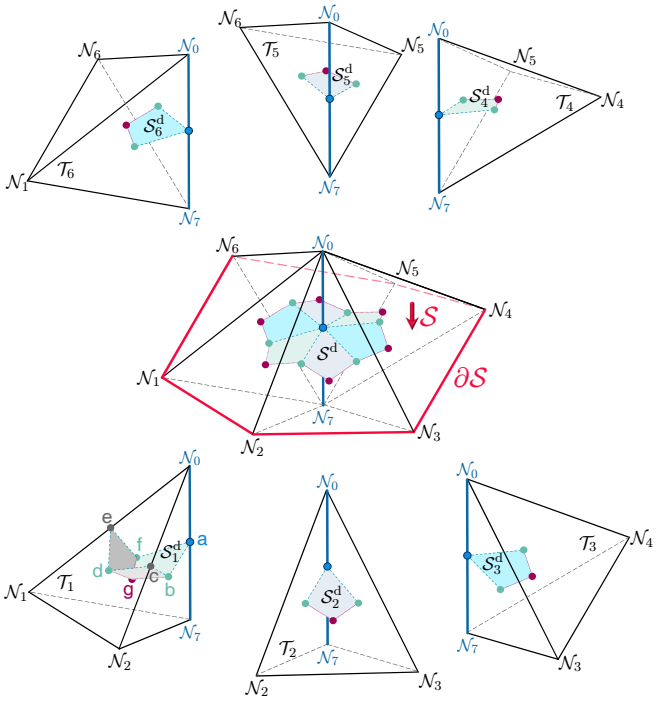

Fig. 1. Simplicial star of an edge and (a part of) its barycentric dual – picture inspired by [10, Fig. 4.17]. The simplicial star consists of the tetrahedra $\mathcal{T}_i$, $i = 1,\ldots,6$, that share the common edge $\overrightarrow{\mathcal{N}_0\mathcal{N}_7}$. The facetted surface $\mathcal{S}^{\mathrm{d}} = \cup_{i=1}^{6}\mathcal{S}_i^{\mathrm{d}}$ is the part of its barycentric dual consisting of the facets meeting at the mid-point of the edge $\overrightarrow{\mathcal{N}_0\mathcal{N}_7}$ (encircled cyan bullet). The elements of S^{d} are: plum bullets = barycentres of the tetrahedra $\mathcal{T}_i$; light-teal bullets = barycentres of the faces $\triangle\mathcal{N}_0\mathcal{N}_7\mathcal{N}_i$; dashed-cyan segments = $\mathcal{S}^{\mathrm{d}}$ edges included in the face $\triangle\mathcal{N}_0\mathcal{N}_7\mathcal{N}_i$; dotted-plum segments = $\mathcal{S}^{\mathrm{d}}$ edges pointing inward the tetrahedra $\mathcal{T}_i$. The picture of $\mathcal{T}_1$ contains all facets of the barycentric dual surface enclosing the node $\mathcal{N}_0$, with gray bullets denoting the mid-points of the edges $\overrightarrow{\mathcal{N}_0\mathcal{N}_1}$ and $\overrightarrow{\mathcal{N}_0\mathcal{N}_2}$. The facetted surface $\mathcal{S}$ consists of the 'upper' faces of the 6 tetrahedra, with $\partial\mathcal{S}$ being its contour.

This strategy, combined with the applicable space-time boundary conditions, results into a time-dependent system of algebraic equations with the expansion coefficients of $\boldsymbol{E}$ and $\boldsymbol{B}$ as unknowns. It is conjectured that the relevant system will be amenable to a time-domain solution via a standard marching-in-time scheme (see [22] for possible alternatives). Due to the problem's complexity, formulating stability criteria will be

‡The present formalism is constructed by assuming exclusively locally and instantaneously reacting media [26, Chapter 19].

quite likely very difficult, with software implementations being expected to provide practical indicators to this end.

VI. Computational costs & programming complexity

The fact that the simplicial stars of edges and, above all, faces are much smaller than those of nodes implies that consistently linear edge and face expansions are computationally much less efficient than Cartesian (nodal) expansions. Moreover our strategy requires the simultaneous discretisation of two quantities (as was the case with the first CEM formulation involving edge and face expansion functions [7]). It is then clear that our method will require calculating a (very) large number of DoFs. On the other hand, the expansion inefficiency is compensated by the fact that interfaces are preserved, this eliminating the need of dense meshing in the vicinity of such interfaces. Moreover, one can consider combining an edge plus face expansion at interfaces with a Cartesian expansion inside domains of homogeneity (as was the case in [16], [21]).

As stated, our method can, in principle, handle surface electric currents and charges. However, this will entail coding complications due to the need to manage incomplete edge and face simplicial stars where jumps must be enforced.

To conclude with, experience with building (general purpose) FEM packages shows that one of the most critical bottlenecks is obtaining quality meshes that are also complemented with adequate topological information and a versatile mapping between geometrical elements and DoFs. The meshing demands are enhanced in the proposed method that requires both a simplicial mesh and its barycentric dual, with full topological information. Addressing these challenges may be facilitated by advances in dual meshing in computer graphics [27] or in mathematics, with [28, Chapters 7 and 8] discussing expedient solutions for associating geometrical elements and DoFs.

Acknowledgment

The authors express their gratitude to Professor Adrianus T. de Hoop, Dr. Gerrit Mur and Professor Enzo Tonti with whom they had the privilege of collaborating, among others for developing some of the methods quoted in this contribution – their physical and mathematical insight underpins the presently advocated technique. A word of gratitude is also due to Professor Thomas Weiland with whom one of the authors had several opportunities of exchanging fruitful ideas – his seminal paper [6] represents a true turning point in CEM.

References

[1] G. W. Hanson, H. Xin, W. C. Chew, N. Engheta, C. Fumeaux, and S. C. Hagness "The role of commercial simulators and multidisciplinary training in graduate-level electromagnetics education," *IEEE Antennas Propag. Mag.*, vol. 59, no. 6, pp. 127–130, Dec. 2017.

[2] P. Mühlschlegel, H.-J. Eisler, O. J. F. Martin, B. Hecht, and D. W. Pohl, "Resonant optical antennas," *SCIENCE*, vol. 308, pp. 1607–1609, Jun. 2005.

[3] B. Khlebtsov, A. Melnikov, V. Zharov, and N. Khlebtsov, "Absorption and scattering of light by a dimer of metal nanospheres: comparison of dipole and multipole approaches," *Nanotechnology*, vol. 17, pp. 1437–1445, Feb. 2006.

[4] A. Cacciola, M. A. Iatî, R. Saija, F. Borghese, P. Denti, O. M. Maragò, and P. G. Gucciardi, "Spectral shift between the near-field and far-field optoplasmonic response in gold nanospheres, nanoshells, homo- and hetero-dimers," *J. Quant. Spectrosc. Radiat. Transfer*, vol. 195, pp. 97–106, Jul. 2017.

[5] Y. Jiang, N. Cucu Laurenciu, and S. D. Cotofana, "On carving basic Boolean functions on graphene nanoribbons conduction maps," in *Proc. ISCAS*, 2018, pp. 1–5. [Online]. doi: 10.1109/ISCAS.2018.8351421.

[6] T. Weiland, "Eine Methode zur Lösung der Maxwellschen Gleichungen für sechskomponentige Felder auf diskreter Basis," *AEÜ*, vol. 31, no. 3, pp. 116–120, Mar. 1977.

[7] G. Mur and A. T. de Hoop, "A finite-element method for computing three-dimensional electromagnetic fields in inhomogeneous media," *IEEE Trans. Magn.*, vol. 21, no. 6, pp. 2188–2191, Nov. 1985.

[8] A. Bossavit, "Whitney forms: a class of finite elements for three-dimensional computations in electromagnetism," *IEE Proc.*, vol. 135, pt. A, no. 8, pp. 493–500, Nov. 1988.

[9] E. Tonti, "Finite formulation of the electromagnetic field," *PIER*, vol. 32, pp. 1–44, 2001.

[10] E. Tonti, *The Mathematical Structure of Classical and Relativistic Physics. A General Classification Diagram*, NY: Birkhuser/Springer, 2013.

[11] A. Bossavit and L. Kettunen, "Yee-Like schemes on staggered cellular grids: A synthesis between FIT and FEM approaches," *IEEE Trans. Magn.* vol. 36, no. 4, pp. 861–867, Jul. 2000.

[12] A. Bossavit, "Mixed-hybrid methods in magnetostatics: Complementarity in one stroke," *IEEE Trans. Magn.*, vol. 39, no. 3, pp. 1099–1102, May 2003.

[13] T. Tarhasaari, L. Kettunen, and A. Bossavit, "Some realizations of a discrete Hodge operator: A reinterpretation of finite element techniques," *IEEE Trans. Magn.*, vol. 35, no. 3, pp. 1494–1497, May 1999.

[14] F. Trevisan and L. Kettunen, "Geometric interpretation of discrete approaches to solving magnetostatic problems," *IEEE Trans. Magn.*, vol. 40, no. 2, pp. 361–365, Mar 2004.

[15] A. T. de Hoop, I. E. Lager, and P. Jorna, "The space-time integrated model of electromagnetic field computation," *Electromagnetics*, vol. 22, no. 5, pp. 371–379, 2002.

[16] I. E. Lager and G. Mur, "Application of the domain-integrated field relations method to the solution of large scale static and stationary magnetic field problems," *IEEE Trans. Magn.*, vol. 38, no. 2, pp. 465–468, Mar. 2002.

[17] I. E. Lager, E. Tonti, A. T. de Hoop, G. Mur, and M. Marrone, "Finite formulation and domain-integrated field relations in electromagnetics - A synthesis," *IEEE Trans. Magn.*, vol. 39, no. 3, pp. 1199–1202, May 2003.

[18] A. Garg, *Classical Electromagnetism in a Nutshell*, New Jersey, NJ: Princeton University Press, 2012.

[19] J.-M. Jin, *The Finite Element Method in Electromagnetics*, 3rd ed., Hoboken, NJ: John Wiley & Sons Inc, 2014.

[20] T. Euler, *Consistent Discretization of Maxwells Equations on Polyhedral Grids*, dissertation, Darmstadt, Germany, Oct. 2007. [Online]. Available: http://tuprints.ulb.tu-darmstadt.de/895/1/Euler_Timo.pdf.

[21] G. Mur, "The finite-element modeling of three-dimensional electromagnetic fields using edge and nodal elements," *IEEE Trans. Antennas Propag.*, vol. 41, no. 7, pp. 948–953, Jul. 1993.

[22] A. Akbarzadeh-Sharbaf and D. D. Giannacopoulos, "Finite-element time-domain solution of the vector wave equation in doubly dispersive media using M obius transformation technique," *IEEE Trans. Antennas Propag.*, vol. 61, no. 8, pp. 4158–4166, Aug. 2013.

[23] Z. Ren and X. Xu, "Dual discrete geometric methods in terms of scalar potential on unstructured mesh in electrostatics," *IEEE Trans. Magn.* vol. 50, no. 2, art. 7000704, Feb 2014.

[24] H. J. W. Müller-Kirsten, *Electrodynamics*, 2nd ed., New Jersey, NJ: World Scientific Publishing Co. Pte. Ltd., 2011.

[25] V. H. Rumsey, "Reaction concept in electromagnetic theory," *Phys. Rev*, vol. 94, no. 6, pp. 1483–1491, Jun. 1954.

[26] A. T. de Hoop, *Handbook of Radiation and Scattering of Waves*, London: Academic Press, 1995; electronic reproduction (with corrections) 2008, freely downloadable, for private use, from http://www.atdehoop.com.

[27] G. Taubin, "Dual mesh resampling," *Graphical Models*, vol. 64, no. 2, pp. 94–113, Mar. 2002.

[28] E. Grinspun and M. Wardetzky (editors), *Discrete Differential Geometry: An Applied Introduction*, [Online]. Available: http://ddg.cs.columbia.edu/SIGGRAPHASIA08/SiggraphAsia2008DDGCourse.pdf.